Mechanical communication through the ECM is frequency-dependent due to cell sensitivity to mechanical signal shape

Ido Nitsan[1], Stavit Drori[1] and Shelly Tzlil[1*]

[1] Faculty of Mechanical Engineering, Technion – Israel Institute of Technology, Haifa 32000 Israel.

* To whom correspondence should be addressed: Email: shellytz@technion.ac.il

Abstract

Cells communicate mechanically by sensing and responding to mechanical deformations generated by their neighbors in the extracellular matrix (ECM). By directly measuring the mechanical coupling between a cardiac cell and an artificial 'mechanical cell' and monitoring the dependence of beat-to-beat variability on mechanical coupling, we can quantify the sensitivity of cardiac cells to mechanical signals. Here we show that due to the dynamic viscoelastic properties of collagen hydrogels (a major component of the cardiac ECM), the shape of the mechanical signal changes in a frequency-dependent manner as it propagates through the gel, resulting in mechanical communication that depends on beating frequency. Moreover, we show that cardiac cell sensitivity to the shape of the mechanical signal results from its responsiveness to the loading rate, with an optimal loading rate for efficient mechanical communication. The dependence of signal shape on ECM viscoelasticity and the existence of an optimal loading rate suggest that there are ideal viscoelastic properties for mechanical communication between cardiac cells.

Introduction

It was recently established that cells are able to communicate mechanically by responding to mechanical deformations generated by their neighbors (1–7). It is a challenging task to measure and define mechanical communication between cells. An additional challenge is to separate the mechanical component of intercellular communication from other modes of communication, such as a change in the amount or type of secreted chemo-attractants. Often, mechanical communication is defined as migration towards a contractile cell or frequency of cell-cell contact formation and mechanical coupling is only qualitatively estimated, for example, by imaging matrix fiber alignment spanning cell pairs (8, 9). In cardiac cells, we have shown previously that mechanical communication is essential for synchronized beating. We have previously shown that spontaneously beating cardiac cells can be paced using a 'mechanical cell', which consist of a tungsten probe that mimics the deformations generated by a neighboring beating cell (1). There is no physical contact between the cell and the probe, and the interaction therefore is purely mechanical and mediated through propagation of deformations in the matrix. In addition, we have measured mechanical coupling directly and showed that beat-to-beat variability decays exponentially with the level of mechanical coupling (3).

The ECM is highly non-linear viscoelastic material and therefore exhibits both elastic and viscous responses in a frequency dependent manner. In high frequencies it behaves as a pure elastic material while in lower frequencies molecular relaxation processes occur within the network and influence material response. Several recent studies have demonstrated the importance of ECM viscoelasticity in determining cell response (10–16). Intermediate viscosity was shown to maximize cell spreading (11) and fast stress relaxation results in robust cell migration on soft substrates (17).

Mechanical cell-cell communication is mediated by the extracellular matrix (ECM) and due to its viscoelasticity, cell-generated deformations will be filtered via the viscoelastic medium and therefore amplified, dissipated, or delayed in a frequency-dependent manner. As a result, the local mechanical signal generated by beating cardiac cells is expected to change its shape, phase, and amplitude in a way that depends on the beating frequency. Using collagen I, the major component of the cardiac ECM, we show that mechanical communication on collagen is frequency dependent. We demonstrate that this dependence results from changes in the mechanical signal shape as it propagates through the matrix. We further show that cell sensitivity to signal shape results from its sensitivity to the loading rate of the mechanical signal with an optimal loading rate of 1μm/sec at a beating frequency of 1Hz.

Results and discussion

<u>Mechanical communication on ECM is frequency-dependent</u>

Primary cardiomyocytes were isolated from neonatal rat hearts and cultured on either polyacrylamide gels or collagen I hydrogels. Hydrogels made of collagen I, a native component of the cardiac ECM, were used to explore the role of the dynamic viscoelastic properties of the ECM. We used glycated collagen matrices (18) with collagen concentration of 5mg/ml and ribose concentration of 250mM, to obtain Young's modulus of ~1 kPa, comparable to the Young's modulus of our polyacrylamide substrate. Substrate stiffness in this range was shown to support optimal cardiac cell beating (19). We recently introduced the experimental setup (1, 3) which is illustrated schematically in Figure 1a. The 'mechanical cell' is a home-built mechanical device which consists of a tungsten probe mounted on a piezo stage with x-y-z actuators. Driven by the actuators, the probe cyclically pulls the substrate towards and away from the cardiac cell. The mechanical probe deforms the substrate such as to mimic the mechanical deformations generated by a neighboring beating cardiac cell. There is no physical

74 contact between the cell and the probe and the interaction therefore is solely mechanical and
75 mediated through propagation of deformations in the underlying substrate.

76 We have recently shown that cardiac cells can be paced mechanically using a 'mechanical cell'
77 (1) and that phase entrainment depends on the level of mechanical coupling (3). Isolated
78 spontaneously beating cardiac cells have large beat-to-beat variability (variability in the time
79 interval between consecutive contractions) that must be reduced to allow for synchronized
80 contraction. In the intact heart, beat-to-beat variability serves as an indicator of cardiac health
81 and increased beat-to-beat variability is associated with higher risks for cardiovascular events.
82 We have recently shown that mechanical coupling regulates beat-to-beat variability (3).

83 By gradually increasing the amplitude of the 'mechanical cell' signal, we control the level of
84 mechanical coupling. We directly measure the mechanical coupling of the cardiac cell to the
85 'mechanical cell' and monitor cardiac cell beat-to-beat variability as a function of mechanical
86 coupling strength for the same cell. We let the cell interact with the probe for ten minutes before
87 recording the signal and changing the amplitude to allow the cell to reach stationary behavior.
88 Quantitatively, beat-to-beat variability of a cardiac cell (ξ) decays exponentially with the
89 strength of mechanical coupling (χ) to either a 'mechanical cell' or a neighboring cardiac cell
90 according to $\xi = ae^{-k(\omega)\chi}$ where k is the exponential decay constant (Figure 1, Videos S1-S2
91 and (3)). The inverse value of the decay constant is the value of mechanical coupling required
92 for the beat-to-beat variability to decay by a factor of 1/e. Therefore, k, can be used as a measure
93 of cell sensitivity to mechanical coupling, or equivalently, as a measure of mechanical
94 communication efficiency. Additional details on the experimental assay and the measurements
95 of beat-to-beat variability and mechanical coupling can be found in the supplementary
96 information (Fig. S1) and in previous work setup (1, 3).
97 In the general case, the exponential decay constant k is expected to depend on the beating
98 frequency of the cardiac cell. However, as shown in Figure 2a-b, on linear elastic materials

99 such as polyacrylamide, the exponential decay constant does not depend on frequency and
100 equals 5.5±0.23. This indicates that on linear elastic materials, cell sensitivity to mechanical
101 coupling is independent of beating frequency.

102 As shown in Figure 2c-d, for collagen hydrogels, the major component of the cardiac ECM,
103 the behavior is qualitatively different. On collagen hydrogels, the decay constant, and therefore
104 mechanical communication efficiency, is frequency-dependent and increases monotonically
105 with the beating frequency within the examined range.

106 ***Cells are sensitive to the shape of the mechanical signal***

107 The nonlinearity and viscoelasticity of collagen are expected to change the shape of the
108 oscillating mechanical signal as it propagates through the matrix. Indeed, a clear frequency-
109 dependent change in the shape of the propagating strain was observed on collagen hydrogels
110 (Figure 3a-b). Collagen fibers are unable to resist compressive strain and are known to buckle
111 under cell-generated compressive forces and reorient along tensile forces (9, 20). Collagen
112 buckling is observed in our experiments as shown in Fig. S2 and Video S2 and can explain the
113 change in signal shape as it propagates through the collagen gel.

114 To test whether the change in shape of the mechanical signal is the origin of the frequency-
115 dependent cell response, we repeated the experiment with a different protocol. As we have
116 shown previously, since polyacrylamide gels are linear elastic gels, there is no apparent change
117 in the shape of the signal while it propagates through the gel. Any signal shape (e.g., sinusoidal
118 form) applied locally in the gel, will keep its form as it propagates in the gel and will have the
119 same shape next to the cell (schematically shown in Figure 2a,3c). We repeat the experiment,
120 but this time, for a given beating cell (e.g., with frequency ω_1), we apply on the polyacrylamide
121 gel an oscillatory signal that matches the shape of the signal observed on collagen at the same
122 frequency (ω_1) next to the cell (after it has propagated through the matrix). This experimental

123 protocol is illustrated schematically in Figure 3c. For example, for a cell beating at 0.3Hz, the
124 'mechanical cell' generates on the polyacrylamide gel a signal with the shape of the red curve
125 in Figure 2c rather than a sinusoidal signal.

126 As clearly shown in Figure 3d, we are able to reproduce the frequency-dependent cell response
127 by mimicking on polyacrylamide the frequency-dependent signal shape observed on collagen.
128 This implies that the frequency-dependent shape of the mechanical signal by itself can explain
129 the change in cell sensitivity to mechanical coupling at different frequencies.

130 ***Mechanical communication is most efficient at an optimal strain rate***

131 As shown in Figure 3d, mechanical coupling efficiency depends on signal shape. Moreover,
132 the signal shape by itself can reproduce the effect of having a viscoelastic material as a
133 substrate. Different signal shapes are associated with different loading rates and it was recently
134 shown that cell response is sensitive to the rate of applied force for fibroblast spreading under
135 cyclic strain (21). To directly test the effect of loading rate on cell sensitivity to mechanical
136 coupling and its ability to communicate mechanically efficiently, we repeat the experiments on
137 polyacrylamide with a set of trapezoid signals. We used trapezoid signals since the loading rate
138 is not constant for a sinusoidal signal whereas trapezoid signals have constant slopes and
139 therefore a well-defined loading rate. All of the trapezoid strain profiles, have the same
140 frequency but different slopes that correspond to different loading rates.

141 As done in the previous set of experiments, we gradually increase the trapezoid-shaped
142 oscillations amplitude of the 'mechanical cell' at a frequency identical to the beating frequency
143 of the cell and monitor beat-to-beat variability as a function of the strength of mechanical
144 coupling. We conducted these experiments on cardiac cells that beat at 1Hz using 1Hz
145 trapezoid signals on polyacrylamide substrates. When increasing the amplitude of the

146 ‘mechanical cell’, we keep the loading rate of the trapezoid signal constant by changing the
147 stall times between rise-and-fall.

148 As clearly shown in Figure 4a, the decay constant (*k*) of the beat-to-beat variability with
149 mechanical coupling, i.e., the sensitivity of cells to mechanical coupling, has a non-monotonic
150 dependence on the loading rate with a maximal value at a loading rate of ~1μm/sec. Therefore,
151 mechanical communication between cardiac cells beating at 1Hz is most efficient when the
152 signal loading rate is ~1μm/sec.

153 To incorporate the results obtained using oscillatory signals on polyacrylamide and collagen
154 substrates at 1Hz (as reported in Figure 2b,d), we use the maximal loading rate of the
155 mechanical signals, since the loading rate for these signals is not constant. As shown in Figure
156 4a, these points fall on the same curve.

157 As a reminder, *k* is the exponential decay constant of beat-to-beat variability as a function of
158 mechanical coupling to a neighboring cell. To demonstrate how suboptimal loading rate,
159 resulting in reduced mechanical coupling efficiency (i.e., a lower k) translates to increased
160 beat-to-beat variability, we show the decrease in beat-to-beat variability as a function of
161 loading rate for a given mechanical coupling of χ=0.1 (Figure 4b). This mechanical coupling
162 strength (χ=0.1) corresponds, for example, to cells contracting at 5% strain on 3kPa PA
163 separated by 80 μm along the axis perpendicular to the contraction direction, (equivalent to a
164 distance of approximately 4-8 cell diameters). As clearly shown in Figure 4b, while beat-to-
165 beat variability is reduced by nearly 80% in the optimal loading rate of 1 μm/sec, it is reduced
166 by only 20% in the lowest or highest loading rates tested (1.73 μm/sec and 0.36 μm/sec
167 respectively).

168

Conclusions

Mechanical communication between cells is mediated by mechanical deformations which propagates through the ECM. Here we show that as the mechanical signal propagates through the ECM, its shape and consequently the associated loading rate is changing, thereby influencing mechanical communication. Modifications to the viscoelasticity of the mechanical environment (for example, by changing the level of enzymatic crosslinking in the ECM or matrix composition), will cause a change in the mechanical signal shape. The existence of an optimal loading rate for mechanical communication, therefore, suggests that there are optimal viscoelastic properties for mechanical communication.

Understanding the dependence of mechanical communication on the dynamic viscoelastic properties of the environment will allow us to tune ECM mechanics in order to achieve synchronized behavior of interacting cells or repair mechanical communication to restore normal function.

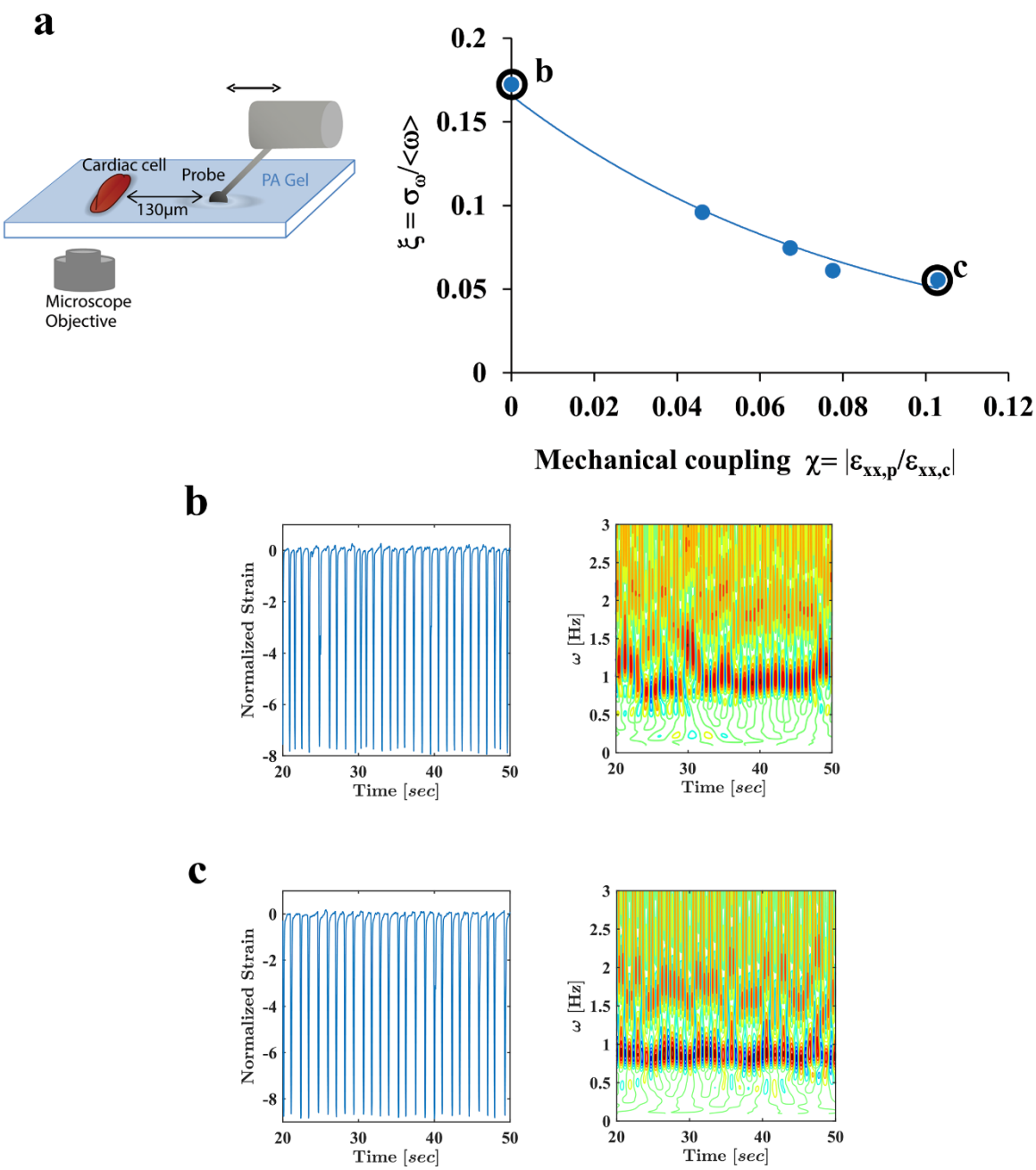

Figure 1: Beat-to-beat variability is reduced exponentially with increased mechanical coupling to a 'mechanical cell': a: *left:* A schematic representation of the 'mechanical cell' setup. A tungsten probe applies an oscillatory strain which mimics the deformations generated by a beating cardiac cell. *Right:* The dependence of beat-to-beat variability, for a representative isolated beating cardiac cell, on the strength of mechanical coupling to a 'mechanical cell'. Beating noise (ξ) decays exponentially with the strength of mechanical coupling (χ) to a 'mechanical cell' according to $\xi = ae^{-k\chi}$ **b:** The normalized strain (*left*) and frequency (*right*)

as a function of time without mechanical coupling, (the point marked in (a) by (b)). **c:** The normalized strain (*left*) and frequency (*right*) as a function of time for a mechanical coupling of χ=0.103. (This point is marked in (a) by (c)).

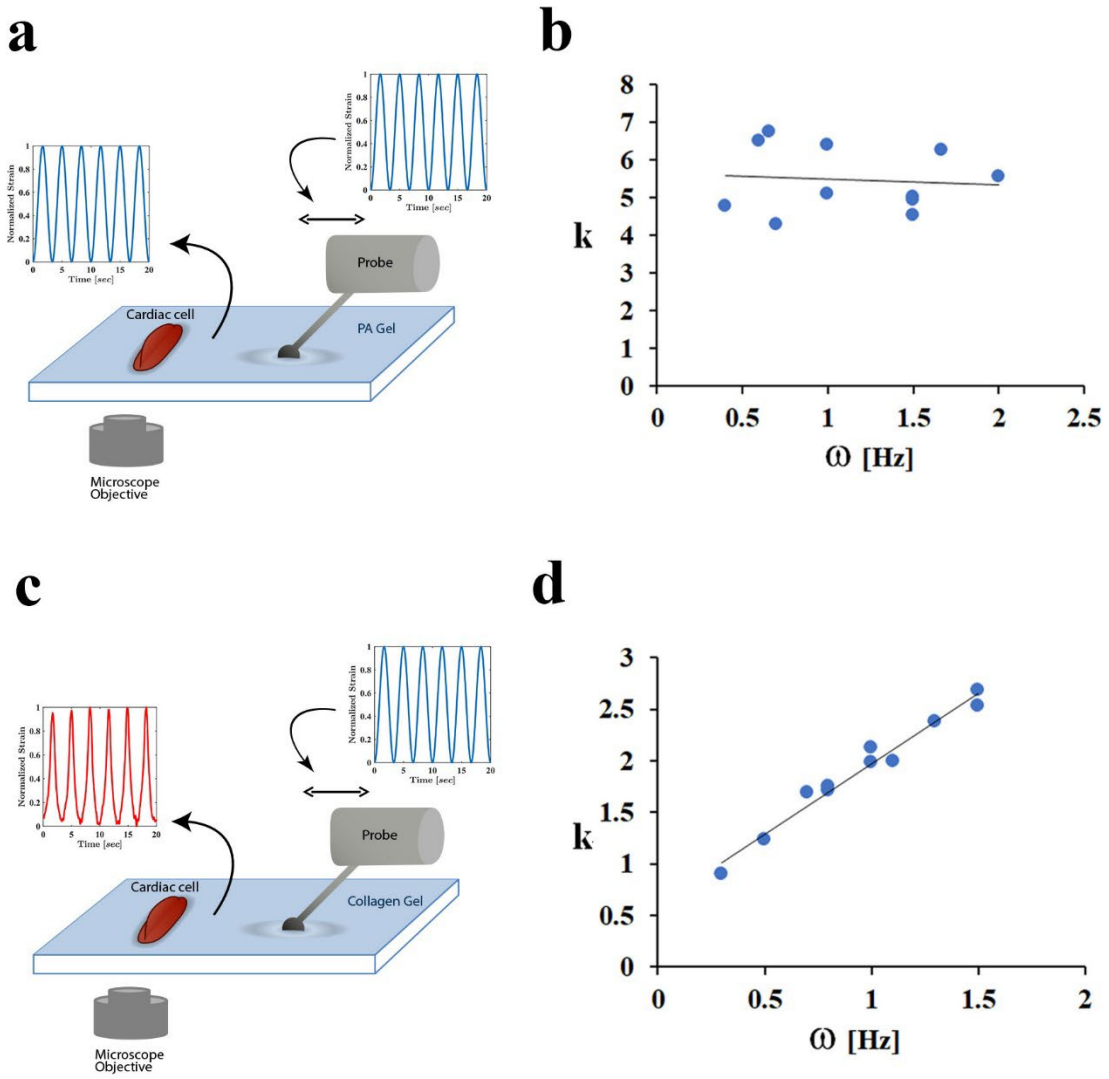

Figure 2: Mechanical communication is frequency-dependent on collagen ECM: a,c: Schematic illustration of the experimental protocols. An isolated cardiac cell interacts mechanically with a 'mechanical cell' on Polyacrylamide (PA) (a) or on collagen (c). The

frequency of 'mechanical cell' oscillations is equal to the average frequency of the beating cardiac cell. A sinusoidal strain signal is applied by the mechanical cell and is measured next to the cell after it propagates through the substrate. On PA substrates (a) the signal still has sinusoidal form next to the cell (keeps its shape as it propagates through the gel). However, on collagen (c), the signal changes its shape as it propagates through the gel.

b,d: Beat-to-beat variability (ξ) decays exponentially with the strength of mechanical coupling (χ) to a 'mechanical cell' according to $\xi = ae^{-k(\omega)\chi}$ (see Figure 1). The decay constant, *k*, is plotted as a function of frequency for isolated cardiac cells interacting with a 'mechanical cell' applying a sinusoidal mechanical signal on polyacrylamide (b) or collagen (d). Notice that the decay constant, *k* does not depend on frequency on polyacrylamide, while there is a strong dependence on frequency on collagen.

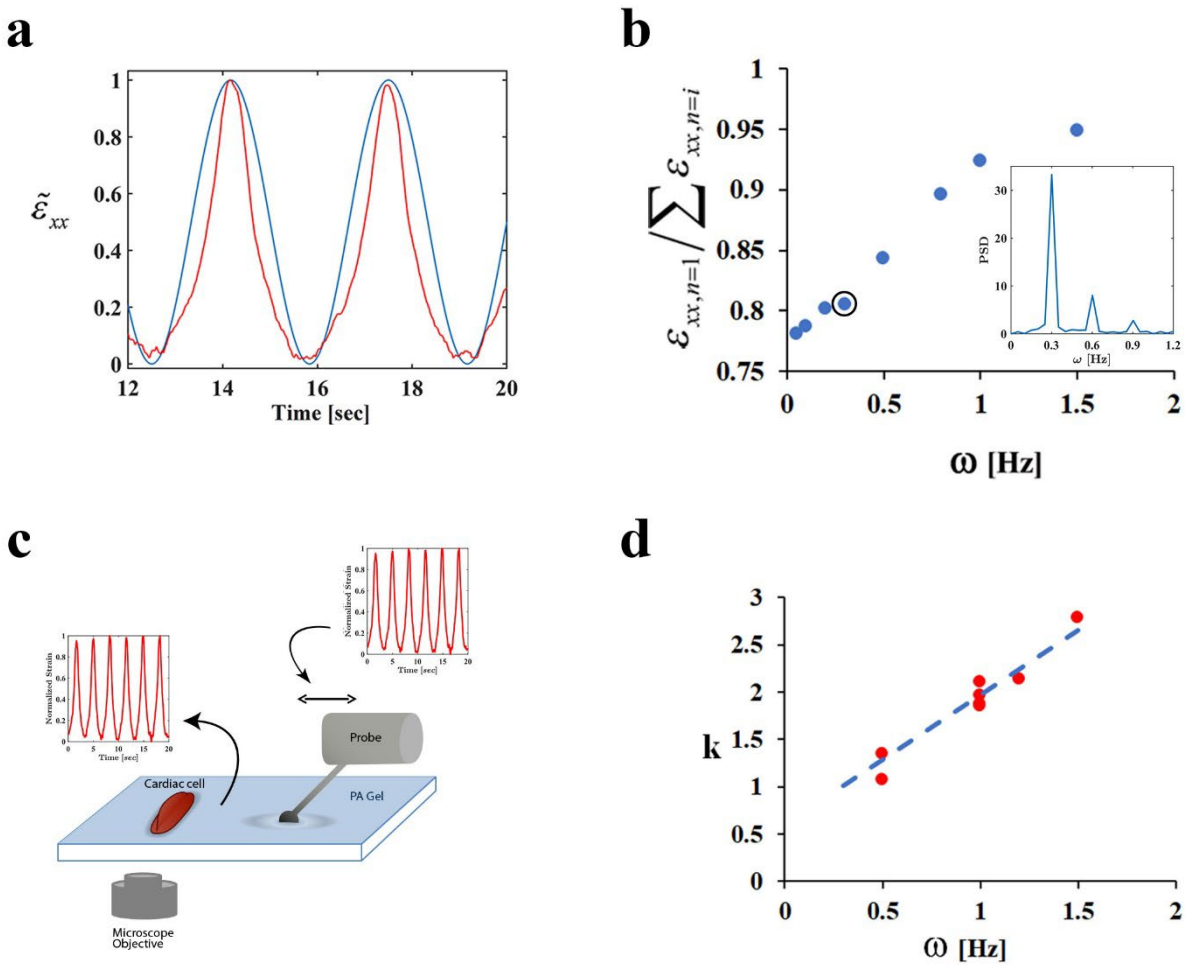

Figure 3: Cells are sensitive to the mechanical signal shape: a: Representative normalized strain signal at 0.3Hz next to the 'mechanical cell' (the location of force application, blue curve) and next to the cell, at a distance of d=84μm from the mechanical cell (after it propagates through the collagen gel ,red curve). **b:** The weight of the first harmonic relative to the harmonic content as a function of frequency, at a distance of d=84μm from the mechanical cell. The marked point corresponds to the red signal in (a) and the corresponding Fourier transform is shown in the inset**. c,d:** Isolated cardiac cells interacting on polyacrylamide with an artificial mechanical cell that applies signals with the frequency-dependent shape observed on collagen next to the cell. c: Schematic illustration of the experimental protocol. d: Beat-to-beat variability (ξ) decays exponentially with the strength of mechanical coupling (χ) to a 'mechanical cell' according to $\xi = ae^{-k(\omega)\chi}$ (see Figure 1). The decay constant, *k*, as a function

222 of frequency for the protocol schematically shown in (c) (red dots). The blue dashed line is the
223 linear fit to the dependence of *k* on frequency for cells on collagen, presented in Figure 2d.
224 Notice that the dependence of the decay constant, *k*, on frequency on collagen can be
225 reproduced by mimicking on polyacrylamide the frequency-dependent signal shapes observed
226 on collagen.

227

228

229

230

231

232

233

234

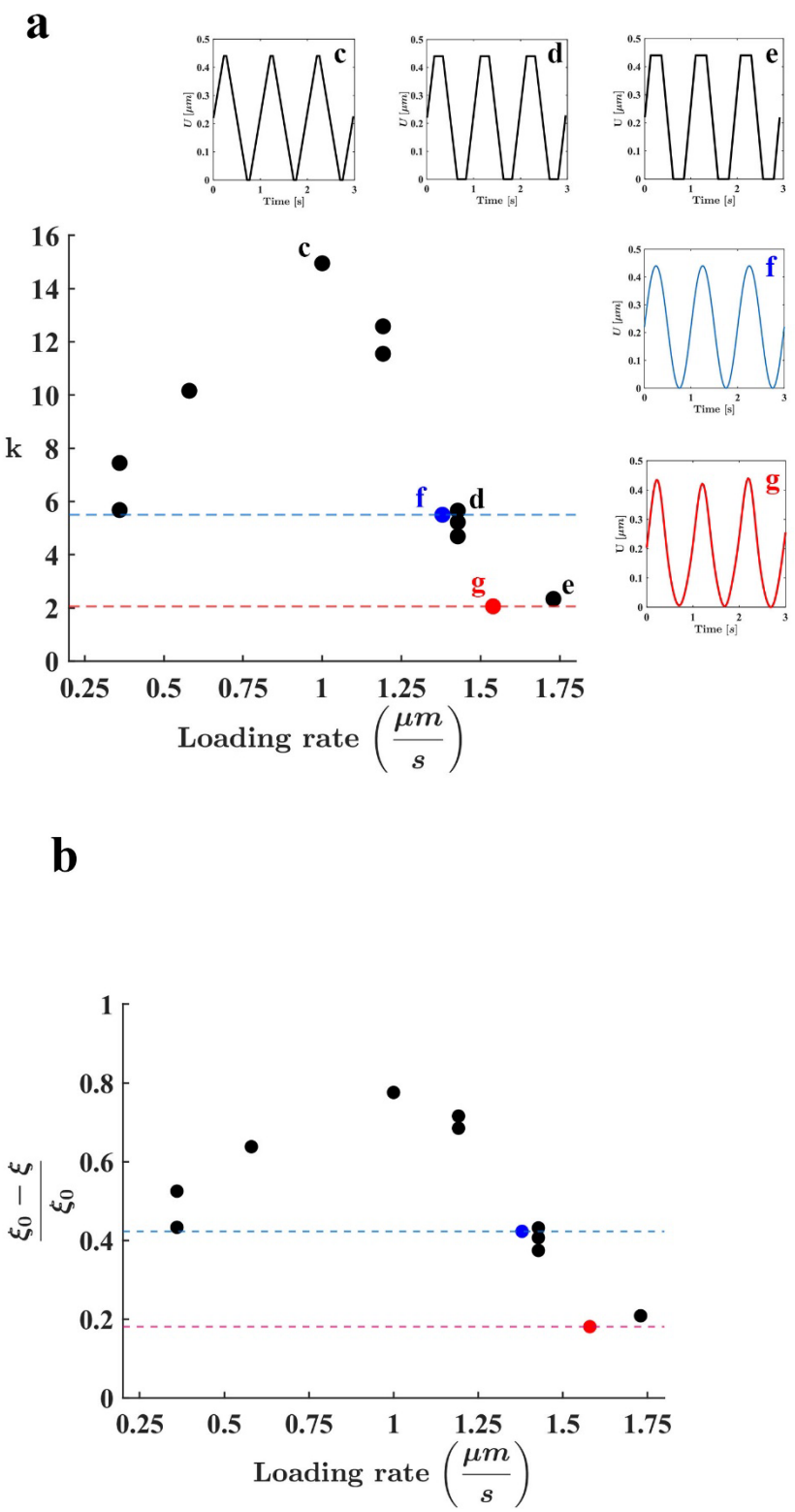

253 **Figure 4: Mechanical communication is loading-rate dependent: a:** Beat-to-beat variability

254 (ξ) decays exponentially with the strength of mechanical coupling (χ) to a 'mechanical cell'

according to $\xi = ae^{-k(\omega)\chi}$ (see Figure 1). The decay constant, *k*, which serves as a measure of cell sensitivity to mechanical coupling (or equivalently, mechanical communication efficiency) is plotted as a function of the loading rate of the mechanical signal for cells interacting with a trapezoid oscillatory signal (●, black circles), an oscillatory sinusoidal signal (●, blue circle) and with an oscillatory signal shape observed on collagen next to the cell at 1Hz (●, red circle). All signals are oscillatory signals applied on polyacrylamide at a frequency of 1Hz. For the non-trapezoid signals, the loading rate is defined as the maximal loading rate, i.e., the maximal derivative of the signal. **c-g:** the mechanical signals generated next to the cells in the points marked by **c-g** in the main graph respectively. k=5.5 and maximal loading rate=1.37 um/s for polyacrylamide; and k=2.1 and maximal loading rate=1.58 um/s for collagen. **b:** The change in beat-to-beat variability (ξ_0-ξ) relative to the initial beat-to-beat variability (ξ_0) as a function of the mechanical signal loading rate for mechanical coupling of χ=0.1.

278 **Materials and Methods**

279 All laboratory procedures conform to the Guide for the Care and Use of Laboratory Animals
280 published by the U.S. National Institutes of Health. Animal usage was approved by the Animal
281 Care and Use Committee of the Technion, Israel Institute of Technology.

282 **Cell culture:** Neonatal cardiomyocytes were isolated from zero-day-old Sprague Dawley (SD)
283 rat pups using the Neonatal Cardiomyocyte Isolation System (Worthington, NJ) according to
284 the manufacturer's instructions as described before(1). Briefly, hearts were rinsed with ice-cold
285 HBSS and trypsinized for 16 hours at 4°C. Following trypsinization, hearts were incubated
286 with trypsin inhibitor at 37°C, and then with collagenase solution for 30 minutes. Cells were
287 triturated, pelleted and resuspended in L15 media (Worthington, NJ). Cells were then subjected
288 to Percoll gradient for separation of cardiomyocytes from non-myocytes. Isolated
289 cardiomyocytes were resuspended with culture media: F10 media (Sigma-Aaldrich, MO)
290 supplemented with 5% fetal calf serum (Biological-Industries, Israel), 5% donor horse serum
291 (Life-technologies, CA), penicillin 10u/ml, streptomycin 0.1mg/ml, 5-Bromo-2'-deoxyuridine
292 (5-BrdU) 0.05mg/ml and $CaCL_2$ 1mM (Signa-Aldrich, MO). Cultured cardiomyocytes were
293 grown for at least 72 hours and up to 6 days.Approximately $8x10^5$ cells were plated on 30mm
294 glass bottom plates (Greiner, Austria) covered with either collagen or matrigel patterned
295 polyacrylamide gels.

296 **PDMS stamp: microfabrication and soft lithography:** The patterns were designed using
297 CleWin 5 (PhoeniX Software, NL). Isolated pairs of rectangles were designed. Rectangles were
298 either 20 x 50um or 20 x 100um. Each rectangle represents a place that will be occupied by a
299 cardiac cell. The distance between two cells in each pair varies throughout the mask (e.g. 10,
300 20, 40, 80, 120um). Chrome masks were manufactured by Delta Mask (Delta Masks BV, NL).
301 A Si master with geometric patterns was fabricated using standard photolithographic technique

302 as previously described(22). PDMS prepolymer was obtained via mixing Silicone elastomer
303 and curing agent at 10:1 ratio (Dow Corning, Midland, MI) and degassing the mixture in a
304 desiccator for 30 min. The prepolymer solution was poured over the Si master mold and cured
305 in the oven at 80°C for 2 h. The elastomeric stamp was then peeled off carefully and cut in 1 ×
306 1 cm^2 squares for micropatterning.

307 **Intermediate patterned glass coverslips:** Either Matrigel or laminin (Corning Inc, NY) was
308 diluted 1:10 in L15 medium (Thermo Fisher). 160µl of the solution was added to the top of
309 elastomeric microstamps, and incubated at 4°C overnight. Following incubation, the solution
310 was aspirated, and the surface of the stamps was dried with a low stream of N_2 gas. The stamps
311 were then used to micropattern clean glass coverslips, via microcontact printing. The stamp
312 was brought into complete conformal contact with a glass coverslip substrate for 5min at room
313 temperature. Small weights (38 g) were placed over the PDMS stamp to aid complete protein
314 pattern transfer from PDMS to intermediate glass

315 **Patterned polyacrylamide plates:** Polyacrylamide (PA) gel coated plates were prepared
316 following the protocol described previously(3). Briefly, 30mm glass bottom plates (Greiner,
317 Austria) were activated using 2% 3-aminopropyltrimethoxysilane and 1% glutaraldehyde
318 solution. Polyacrylamide/Bis-acrylamide 7.5/0.03% solution was mixed with 0.02%
319 suspension of carboxylated dark red fluospheres (Life Technologies), 0.05% Ammonium
320 Persulfate and 0.4% Temed (Bio-Rad, CA). 7.5 µl of mixed PA solution was applied on each
321 activated plate and covered with, matrigel patterned glass coverslip, to form a thin film. The
322 patterned matrigel on the coverslips was transferred to the surface of the polyacrylamide
323 substrates during gelation. Films were left to polymerize for 30 min in room temperature.
324 Following polymerization, polyacrylamide substrates were incubated in phosphate-buffered
325 saline for at least 1 h and the top coverslips were carefully removed with a razor blade(23)

326 **Preparation of collagen coated dishes**: Corning's collagen I (HC) solution was glycated
327 before gel formation. Collagen solution was mixed with ribose in 0.1% acetic acid to final
328 concentration of 250mM ribose, and incubated for 5 days at $4°C$ as previously described(24).
329 Glycated collagen gel coated plates were prepared according to manufacturer protocol
330 (Corning's coating procedure)(25). 30mm glass bottom plates (Greiner, Austria) were activated
331 using 2% 3-aminopropyltrimethoxysilane, and 1% glutaraldehyde solution. 25 μl of glycated
332 collagen solution was applied on each activated plate and covered with the 18mm round glass
333 coverslip, to form a thin film. Films were incubated in $37°C$ 1 hour gelation.

334 **Labeling collagen fibers**: Collagen fibers were labeled using NHS-Rhodamine in a mole
335 ratio of 1:14, for 2 hours on ice. Non-reacted NHS-Rhodamine was removed by dialysis in
336 16.65M acetic acid

337 **Spinning disc confocal microscopy:** Imaging was done using a Nikon Ti-E inverted
338 microscope equipped with two Evolve EMCCD cameras (Photomatrix), 4 laser lines
339 (405,491,561,642), phase contrast and Yokagawa spinning disc confocal. The dish was
340 maintained at 37 ºC with 5% CO_2/95% air using a cage incubator (Okolab). Imaging was done
341 using 40x 0.95 NA (air) PlanApo Lambda objective (Nikon). Fluorospheres were excited using
342 642nm laser (Vortran) and Lifeact-RFP was excited with 561nm laser (Cobolt). Lifeact
343 imaging was done using 100x 1.49 NA oil objective (Nikon).

344 **Mechanical probe assay:** A rigid Tungsten probe with 25um tip diameter (Signatone) was
345 mounted on a three axes (X-Y-Z) micro-positioning stages (Thorlabs) installed on a custom
346 made adaptor for the microscope stage. The probe's tip is immersed into the culture medium
347 and slightly indents the PA substrate (2um indentation) 130um away from the target cell as
348 previously described(1). By gradually increasing the amplitude of probe oscillations, the
349 beating noise of a spontaneously beating cardiac cell can be monitored as a function of the

strength of mechanical interaction with the mechanical probe. We let the cell interact with the probe for 10 minutes before recording the signal and changing the amplitude to allow the cell to reach stationary behavior. Probe oscillation frequency is chosen to be equal to cell frequency in order to separate the effect of pacing from that of noise reduction.

Supplementary information is available.

Acknowledgements: This work was supported by the Israel Science Foundation grants 507/18 and 1009/23.

Author contributions: S.T designed research and wrote the manuscript. I.N. and S.D. performed experiments, I.N and S.T. analyzed the data, S.T. supervised the research. All authors discussed and helped prepare the manuscript.

Competing interests:

The authors declare no competing interests

374 **References**

375 1. I. Nitsan, S. Drori, Y. E. Lewis, S. Cohen, S. Tzlil, Mechanical communication in cardiac cell
376 synchronized beating. *Nat Phys* **12**, 472–477 (2016). DOI:10.1038/nphys3619.

377 2. T. E. Angelini, E. Hannezo, X. Trepat, J. J. Fredberg, D. A. Weitz, Cell Migration Driven by
378 Cooperative Substrate Deformation Patterns. *Phys Rev Lett* **104**, 168104 (2010).

379 3. H. Viner, I. Nitsan, L. Sapir, S. Drori, S. Tzlil, Mechanical Communication Acts as a Noise Filter.
380 *iScience* **14** (2019). DOI:10.1016/j.isci.2019.02.030.

381 4. C. A. Reinhart-King, M. Dembo, D. A. Hammer, Cell-Cell Mechanical Communication through
382 Compliant Substrates. *Biophys J* **95**, 6044–6051 (2008). DOI:10.1529/biophysj.107.127662.

383 5. K. K. Chiou, J. W. Rocks, C. Y. Chen, S. Cho, K. E. Merkus, A. Rajaratnam, P. Robison, M.
384 Tewari, K. Vogel, S. F. Majkut, B. L. Prosser, D. E. Discher, A. J. Liu, Mechanical signaling
385 coordinates the embryonic heartbeat. *PNAS* **113**, 8939–8944 (2016).
386 DOI:10.1073/pnas.1520428113.

387 6. C. Yang, X. Dong, B. Sun, T. Cao, R. Xie, Y. Zhang, Z. Yang, J. Huang, Y. Lu, M. Li, X. Wang, Y. Xu,
388 F. Ye, Q. Fan, Physical immune escape: Weakened mechanical communication leads to
389 escape of metastatic colorectal carcinoma cells from macrophages. *Proceedings of the*
390 *National Academy of Sciences* **121**, e2322479121 (2024). DOI:10.1073/PNAS.2322479121.

391 7. X. Tang, P. Bajaj, R. Bashir, T. A. Saif, How far cardiac cells can see each other mechanically.
392 *Soft Matter* **7**, 6151–6158 (2011). DOI:10.1039/c0sm01453b.

393 8. C. D. Davidson, F. S. Midekssa, S. J. DePalma, J. L. Kamen, W. Y. Wang, D. K. P. Jayco, M. E.
394 Wieger, B. M. Baker, Mechanical Intercellular Communication via Matrix-Borne Cell Force
395 Transmission During Vascular Network Formation. *Advanced Science* **11** (2024).
396 DOI:10.1002/advs.202306210.

397 9. X. Chen, D. Chen, E. Ban, K. C. Toussaint, P. A. Janmey, R. G. Wells, V. B. Shenoy,
398 Glycosaminoglycans modulate long-range mechanical communication between cells in
399 collagen networks. *Proceedings of the National Academy of Sciences of the United States of*
400 *America* **119** (2022). DOI:10.1073/PNAS.2116718119/FORMAT/EPUB.

401 10. O. Chaudhuri, L. Gu, D. Klumpers, M. Darnell, S. A. Bencherif, J. C. Weaver, N. Huebsch, H.-P.
402 Lee, E. Lippens, G. N. Duda, D. J. Mooney, Hydrogels with tunable stress relaxation regulate
403 stem cell fate and activity. *Nature Materials* **15**, 326–334 (2016). DOI:10.1038/NMAT4489.

404 11. Z. Gong, S. E. Szczesny, S. R. Caliari, E. E. Charrier, O. Chaudhuri, X. Cao, Y. Lin, R. L. Mauck, P.
405 A. Janmey, J. A. Burdick, V. B. Shenoy, Matching material and cellular timescales maximizes
406 cell spreading on viscoelastic substrates. *Proceedings of the National Academy of Sciences of*
407 *the United States of America* **115**, E2686–E2695 (2018).
408 DOI:10.1073/PNAS.1716620115/SUPPL_FILE/PNAS.201716620SI.PDF.

409 12. O. Chaudhuri, L. Gu, M. Darnell, D. Klumpers, S. A. Bencherif, J. C. Weaver, N. Huebsch, D. J.
410 Mooney, Substrate stress relaxation regulates cell spreading. *Nature Communications* **6**
411 (2015). DOI:10.1038/ncomms7365.

13. O. Chaudhuri, J. Cooper-White, P. A. Janmey, D. J. Mooney, V. B. Shenoy, Effects of extracellular matrix viscoelasticity on cellular behaviour. *Nature 2020 584:7822* **584**, 535–546 (2020). DOI:10.1038/s41586-020-2612-2.

14. A. Elosegui-Artola, A. Gupta, A. J. Najibi, B. R. Seo, R. Garry, C. M. Tringides, I. de Lázaro, M. Darnell, W. Gu, Q. Zhou, D. A. Weitz, L. Mahadevan, D. J. Mooney, Matrix viscoelasticity controls spatiotemporal tissue organization. *Nature Materials* **22** (2023). DOI:10.1038/s41563-022-01400-4.

15. W. Fan, *et al.*, Matrix viscoelasticity promotes liver cancer progression in the pre-cirrhotic liver. *Nature* **626** (2024). DOI:10.1038/s41586-023-06991-9.

16. J. P. Winer, S. Oake, P. A. Janmey, Non-Linear Elasticity of Extracellular Matrices Enables Contractile Cells to Communicate Local Position and Orientation. *PLoS ONE* **4**, e6382 (2009). DOI:10.1371/journal.pone.0006382.

17. K. Adebowale, Z. Gong, J. C. Hou, K. M. Wisdom, D. Garbett, H. Lee, S. Nam, T. Meyer, D. J. Odde, V. B. Shenoy, O. Chaudhuri, Enhanced substrate stress relaxation promotes filopodia-mediated cell migration. *Nature Materials 2021 20:9* **20**, 1290–1299 (2021). DOI:10.1038/s41563-021-00981-w.

18. M. S. Hall, F. Alisafaei, E. Ban, X. Feng, C.-Y. Hui, V. B. Shenoy, M. Wu, Fibrous nonlinear elasticity enables positive mechanical feedback between cells and ECMs. *Proceedings of the National Academy of Sciences of the United States of America* **113**, 14043–14048 (2016). DOI:10.1073/pnas.1613058113.

19. A. J. Engler, C. Carag-Krieger, C. P. Johnson, M. Raab, H. Y. Tang, D. W. Speicher, J. W. Sanger, J. M. Sanger, D. E. Discher, Embryonic cardiomyocytes beat best on a matrix with heart-like elasticity: scar-like rigidity inhibits beating. *J Cell Sci* **121**, 3794–3802 (2008).

20. Y. L. Han, P. Ronceray, G. Xu, A. Malandrino, R. D. Kamm, M. Lenz, C. P. Broedersz, M. Guo, Cell contraction induces long-ranged stress stiffening in the extracellular matrix. *Proceedings of the National Academy of Sciences* **115**, 4075–4080 (2018). DOI:10.1073/PNAS.1722619115.

21. I. Andreu, B. Falcones, S. Hurst, N. Chahare, X. Quiroga, A.-L. Le Roux, Z. Kechagia, A. E. M. Beedle, A. Elosegui-Artola, X. Trepat, R. Farré, T. Betz, I. Almendros, P. Roca-Cusachs, The force loading rate drives cell mechanosensing through both reinforcement and cytoskeletal softening. *Nature Communications 2021 12:1* **12**, 1–12 (2021). DOI:10.1038/s41467-021-24383-3.

22. X. Tang, M. Yakut Ali, M. T. A. Saif, A novel technique for micro-patterning proteins and cells on polyacrylamide gels. *Soft Matter* **8**, 7197 (2012). DOI:10.1039/c2sm25533b.

23. A. J. S. Ribeiro, Y.-S. Ang, J.-D. Fu, R. N. Rivas, T. M. A. Mohamed, G. C. Higgs, D. Srivastava, B. L. Pruitt, Contractility of single cardiomyocytes differentiated from pluripotent stem cells depends on physiological shape and substrate stiffness. *Proceedings of the National Academy of Sciences* **112**, 12705–12710 (2015). DOI:10.1073/pnas.1508073112.

24. R. Roy, A. Boskey, L. J. Bonassar, Processing of type I collagen gels using nonenzymatic glycation. *J Biomed Mater Res A* **9999A**, NA-NA (2009). DOI:10.1002/jbm.a.32231.

25. , Corning collagen I coating procedures, https://certs-ecatalog.corning.com/life-sciences/certs/354249/354249_9343002.pdf (October 11, 2022).

453